Journal of the European Ceramic Society **6** (1990) 53–64

Thermodynamic Calculations of Si–C–O Fiber Stability in Ceramic Matrix Composites

Peter Greil

Technische Universität Hamburg–Harburg, Arbeitsbereich Technische Keramik,
Harburger Schloßstr. 20, D-2100 Hamburg 90, FRG

(Received 9 January 1990; accepted 20 February 1990)

Abstract

Thermochemical fiber degradation reactions of multiphase Si–C–O fibers in inert (Ar) and oxidic (air) atmosphere as well as single-phase C and SiC fibers in various carbide, nitride and oxide matrices were calculated in the temperature range 1000–2000°C. The calculations indicate a greater stability of the single-phase SiC as compared to the C fiber in all matrices. The C fiber is fairly stable in AlN and Al_2O_3 *matrix. The silicon carbide fiber is stable in AlN and* Si_3N_4 *as well as in* Al_2O_3 *and* SiO_2*. Above critical temperatures metal carbides are formed at the fiber–matrix interface. An attempt was made to define boundary conditions for the fabrication of fiber-reinforced ceramic matrix composites.*

Die thermochemischen Zersetzungsreaktionen mehrphasiger S–C–O Fasern in inerter (Ar) und oxidierender (Luft) Atmosphäre sowie einphasiger C und SiC Fasern in verschiedenen Carbid-, Nitrid- und Oxid-Matrixwerkstoffen wurden im Bereich 1000–2000°C berechnet. Die Berechungen ergaben für alle Grundwerkstoffe eine höhere Beständigkeit der einphasigen SiC Faser verglichen mit der C Faser. Die C Faser ist in einer AlN und Al_2O_3 *Matrix relativ stabil. Die Siliziumcarbidfaser ist in AlN und* Si_3N_4 *aber auch in* Al_2O_3 *und* SiO_2 *beständig. Jenseits kritischer Temperaturen bilden sich Metallcarbide an der Faser–Matrix Grenzfläche. Es wurde versucht, für die Herstellung faserverstärker Verbundwerkstoffe mit Keramikmatrix relevante Rahmenbedingungen anzugeben.*

On a calculé les réactions de dégradation thermochimique de fibres multiphasées Si–C–O en atmosphère inerte (Ar) et oxydante (air), ainsi que celles de fibres monophasées de C et de SiC dans différentes matrices carbures, nitrures et oxydes pour des températures comprises entre 1000 et 2000°C. Ces calculs prédisent que la fibre monophasée de SiC est plus stable que celle de C dans toutes les matrices. La fibre de C est assez stable dans les matrices d'AlN et d'Al_2O_3*. La fibre de carbure de silicium est stable dans AlN et* Si_3N_4*, ainsi que dans* Al_2O_3 *et* SiO_2*. Au-delà d'une certaine température, des carbures métalliques se forment à l'interface fibre–matrice. On a tenté de définir les conditions limites de fabrication de composites à matrice céramique renforcée par des fibres.*

1 Introduction

In addition to the families of existing fiber-reinforced polymer–matrix composites (PMCs) and, more recently, the metal–matrix composites (MMCs), newly developed ceramic–matrix composites (CMCs) are now available for potential demonstration applications. A high strength combined with excellent toughness and in particular the environmental stability and low density of the CMCs make them particularly attractive for aerospace applications. The candidate systems are composed of alumina, mullite, silicon carbide, silicon nitride and glass ceramics as matrices and carbon, silicon carbide, alumina and aluminium-silicates as fibers.[1] The development of various high-strength polycrystalline SiC fibers[2,3] especially (Table 1) has stimulated extensive work on the fabrication technology of high temperature resistant fiber-reinforced CMCs.[4–7]

The criteria for the design of CMC systems with the desired property combinations primarily refer to the elastic moduli and the coefficient of thermal expansion of the fiber and matrix components. It is

Journal of the European Ceramic Society 0955-2219/90/$3·50

Table 1. Specifications of various silicon carbide fibers

Trade name	*Manufacturer*	*Composition (mass percent)*	*Tensile strength (MPa)*	*Reference*
Nicalon	Nippon Carbon, Tokyo	59Si, 31C, 10O	2 500–3 300	3
Nicalon LM-202	Nippon Carbon, Tokyo	54Si, 30C, 12O	1 550	29
SCS-6	Avco, Wilmington, MA	SiC on C core	3 920	3
Tyranno	UBE, Tokyo	Si, C, O, 2Ti	>2 970	3
MPS	Dow Corning, Midland, MI	69Si, 30C, 1O	1 050–1 400	3
MPDZ	Dow Corning, Midland, MI	47Si, 30C, 15N, 8O	1 750–2 100	3
HPZ	Dow Corning, Midland, MI	59Si, 10C, 28N, 3O	2 100–2 450	3
MPZ	Dow Corning, Midland, MI	60Si, 2C, 33N, 2O		44

the thermochemical stability of the fiber and the fiber–matrix system, however, which restricts the number of potential systems. For example, the thermal instability of the polycrystalline SiC fiber Nicalon at temperatures above 1000°C has prevented the prolonged use of composites at higher temperatures.[8] Because of the high processing temperatures, generally above 1000°C, which are required for the matrix formation in CMCs by hot-passing, sintering and chemical vapor or melt infiltration, fiber stability versus thermal or chemical degradation has become a key aspect for the design of new composite materials. Thus, intrinsic fiber degradation or extrinsic fiber–matrix reactions which take place at the high fabrication temperature or during long exposure to elevated service temperatures may impede or prevent the aquisition of the desired interface. In particular the fiber–matrix interface structure, which is recognized as a decisive factor for controlling the elasto-mechanical properties of the CMC,[9–12] can only be modified when the thermodynamic and kinetic behavior of the system is known. Thus, coating of the fiber with diffusion barriers, reaction inhibitors or low shear strength layers, in-situ segregation of impurities or precipitation of degradation products at the fiber–matrix interface and solid solution or compound formation may drastically change the composite properties.[13–15]

It is therefore of particular importance to understand the chemical stability of the system constituents in order to improve the material processing and application under severe environmental conditions. While experimental studies were carried out on the thermal stability of polycrystalline SiC fibers,[16–18] a thermodynamic approach was used to explain the interface formation in various fiber–matrix systems.[19–21] This work presents the results of equilibrium phase calculations of Si–C–O fibers in Ar and air as well as incorporated in various carbide, nitride and oxide matrices. Although the thermodynamics may not take into account the kinetics of any degradation reaction the response of the system to a temperature change may indicate critical temperatures at which the fiber degradation reactions will become important. Thus, the optimization of fabrication conditions to obtain stable fiber–matrix composites and the disclosure of 'unreasonable' fiber–matrix combinations may be possible.

2 Thermodynamic Calculations

The computer program EQUITHERM (VCH Verlag, Weinheim, FRG)[22] which is based on the SOLGASMIX program[23] was used to calculate the equilibria phase compositions for a given fiber–matrix system. The program is based on the minimization of the Gibbs free energy, G, as a function of the chemical potential, μ_i, and the amount, n_i, of the ith substance

$$G = (\textstyle\sum \mu_i n_i)_{T,P} \qquad (1)$$

while external variables such as temperature, T, and pressure, P, are kept constant and mass balance is satisfied

$$\sum_j a_{ji} n_i = b_j \qquad j = 1, 2 \dots N$$
$$n_i \geq 0 \qquad i = 1, 2 \dots M \qquad (2)$$

where a_{ji} is the constitution coefficient of the jth substance, b_j is the fixed number of moles of the ith element in the system, M and N are the total numbers of substances and elements in the system, respectively.[24] The chemical potential, μ_i, is given as

$$\mu_i = \mu_i^0 + RT \ln a_i \qquad (3)$$

where a_i is the activity. For ideal gaseous mixed phases $a_i = X_i P$, while for ideal condensed mixed phases $a_i = X_i$ ($a_j = 1$ for stoichiometric phases and hence $\mu_i = \mu_i^0$) with X_i being the mole fraction of the

Table 2. Standard Gibbs free energy data, G^0, at 1273, 1773 and 2273 K after Ref. 25 (reference state of elements: N_2 and O_2 ideal gases; C and Si solids crystalline at 298·15 K, 0·1 MPa)

Species	G^0 (*Jmol*$^{-1}$)		
	At 1 273 K	*At 1 773 K*	*At 2 273 K*
Condensed species			
C	−20 154·978	−37 163·927	−57 624·822
Si	−44 236·194	−73 612·914	−107 198·826
SiC	−127 584·918	−170 212·507	−220 370·642
SiO_2	−1 015 979·252	−1 089 787·535	−1 174 117·356
Si_3N_4	−995 984·665	−1 164 160·2	−1 358 387·336
TiC	−253 645·991	−303 946·645	−362 381·793
TiN	−416 603·982	−471 336·404	−534 113·771
TiO_2	−1 066 599·731	−1 148 378·421	−1 241 320·210
AlN	−378 607·753	−423 912·898	−476 396·857
Al_2O_3	−1 831 495·106	−1 948 429·124	−2 084 589·479
Gaseous species			
CO	−388 618·589	−513 035·403	−642 562·976
N_2	−270 170·688	−391 309·219	−517 511·869
O_2	−288 617·318	−417 857·138	−552 405·922
SiO	−398 103·397	−531 306·419	−669 807·105

*i*th substance in the mixed phase. The chemical potentials in the standard state, $\mu_i^0(T) = G^0(T)$, were calculated according to the the Gibbs–Helmholtz equation from enthalpy and entropy values by integrating a temperature-dependent specific heat function from 298·15 K up to the reaction temperature. Table 2 shows the tabulated values of G^0 at 1273, 1773 and 2273 K[25] for ten condensed and four gaseous substances (plus Ar) which were considered in the calculations.

Assuming mass balance (eqn (2)) the program EQUITHERM solves the optimization problem as expressed by eqn (1) using the Lagrange multiplication method to find the extreme values of the Gibbs free energy surface as a function of the composition of the mixture. The results are represented as phase amount diagrams for a special bulk composition where the proportions of the condensed and gaseous substances present in the mixture are given as mole fraction versus temperature (equivalent to phase stability or Pourbaix diagrams). Small changes in composition, however, may result in pronounced changes of the phase assemblages.[26] The results given in the phase amount diagrams are therefore only strictly valid for the particular composition chosen. For the calculation a closed system containing three multicomponent phases, i.e. the fiber, f, the matrix, m, and gas phase, g, was assumed

$$\sum X_f + \sum X_m + \sum X_g = 1 \tag{4}$$

To account for the fiber degradation at temperature T all condensed reaction products resulting from fiber–matrix reaction at the phase boundary, b, were included in the proportion of the matrix phase

$$(\sum X_m)_T = \sum X_m + \sum X_b \tag{5}$$

and hence

$$(\sum X_f)_T = \sum X_f - \sum X_b \tag{6}$$

Plotting $(\sum X_f)_T$ versus temperature in the phase amount diagrams, all fiber decomposition or fiber–matrix reactions resulted in a decrease in the proportion of the fiber.

3 Results and Discussion

3.1 Si–C–O fiber degradation

The degradation reactions of three different fiber compositions

70 SiC, 20 SiO_2, 10 C (wt%)
75 SiC, 25 SiO_2 (wt%)
80 SiC, 20 C (wt%)

in the Si–C–O system were considered in inert (Ar) and oxidic (air) atmosphere in the temperature range 1000–2000°C. The first composition corresponds to the Nicalon fiber and the last to the Avco monofilament (Table 1) both of which are widely used as reinforcing components in various non-oxide and oxide matrices.[4–7] Figure 1((a) to (c)) shows the phase amount diagrams of both the condensed and gaseous phases and the gas phase only in Ar. Except for the oxygen-free fiber (Fig. 1(c)) the other two fibers are unstable in Ar in the temperature range 1000–2000°C. The oxygen-containing fibers decompose to gaseous SiO and CO at temperatures above 1000°C, resulting in a surface degradation. In the fiber containing free carbon (Fig. 1(a)) CO is the

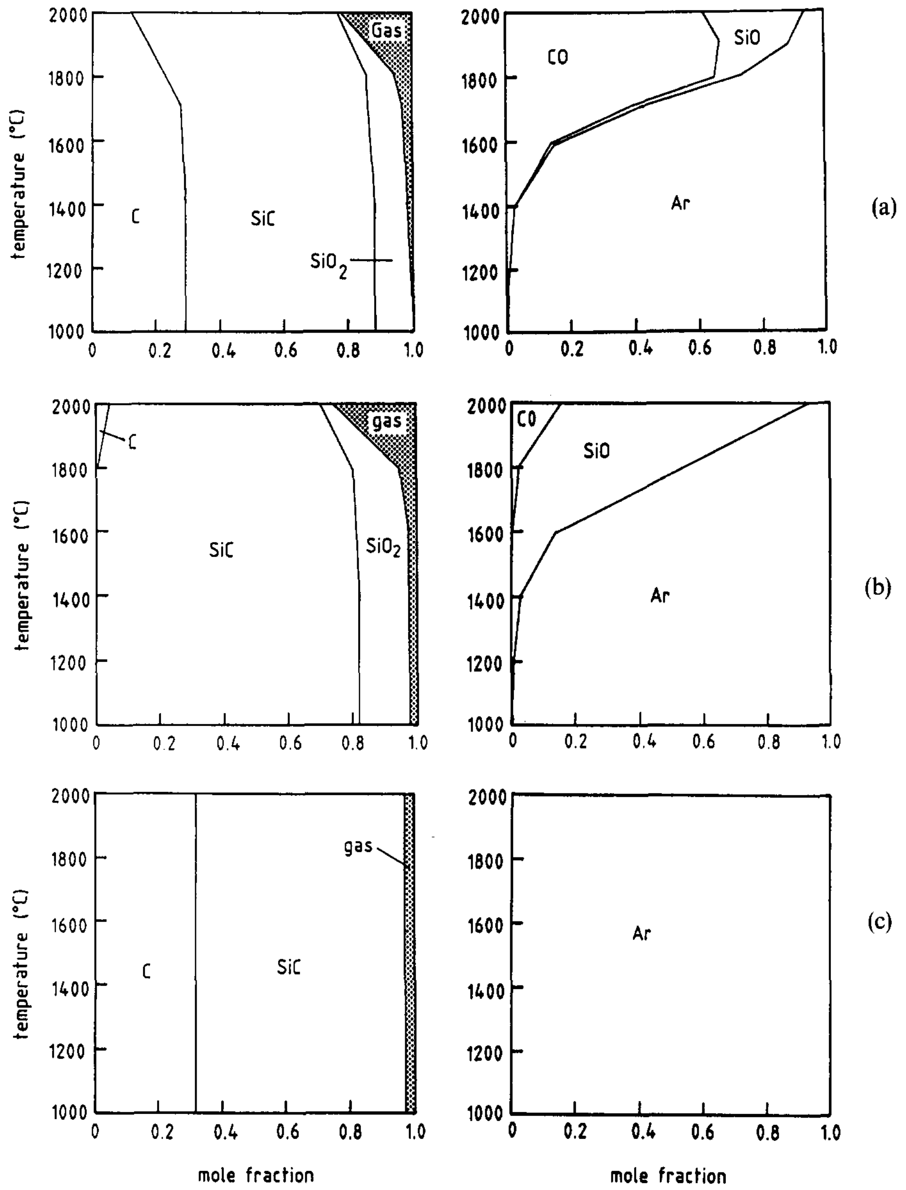

Fig. 1. Phase amount diagrams of the overall phase composition (left) and gaseous phase composition (right) of Si–C–O fibers in Ar atmosphere. (a) 3·8 SiC + 1·8 C + 0·7 SiO_2 + 0·1 Ar; (b) 3·8 SiC + 0·7 SiO_2 + 0·1 Ar; (c) 3·8 SiC + 1·8 C + 0·1 Ar.

dominating gas species at all temperatures according to the reaction

$$3\langle C\rangle + \langle SiO_2\rangle \rightarrow \langle SiC\rangle + 2(CO) \qquad (7)$$

The release of CO was confirmed by mass spectrometry of the evaporating species when Nicalon fibers were heated in vacuum to 1000°C.[16] At higher temperatures SiO additionally occurs

$$\langle SiC\rangle + [SiO_2] \rightarrow \langle C\rangle + 2(SiO) \qquad (8)$$

where $\langle\ \rangle$ denotes solid, [ ], liquid and ( ), gaseous states of matter.

Calculations of the partial pressures of the gaseous substances by taking into account the different activities, a_i, of the ith substance in the crystalline and amorphous states indicated a significant influence of the fiber microstructure on the CO partial pressure but only a minor effect on the SiO partial pressure.[27] The CO partial pressure approaches 0·1 MPa around 1500°C for the case of crystalline Si–C–O fiber which is raised by 200°C for the case of completely amorphous fiber microstructure. The partial pressure of SiO is approximately 2–4 orders of magnitude smaller than that of CO.

In the fiber without free carbon (Fig. 1(b)) SiO is supposed to be the major gas species

$$\langle SiC\rangle + 2\langle SiO_2\rangle \rightarrow \langle CO\rangle + 3(SiO) \qquad (9)$$

In the presence of free carbon an upper limit for the fiber stability of approximately 1500°C was deduced from thermodynamic analysis of the C–SiC–SiO_2 system.[28] At these temperatures the total gas pressure at equilibrium conditions was calculated to exceed 0·1 MPa. Significantly lower gas pressures and thus stability up to approximately

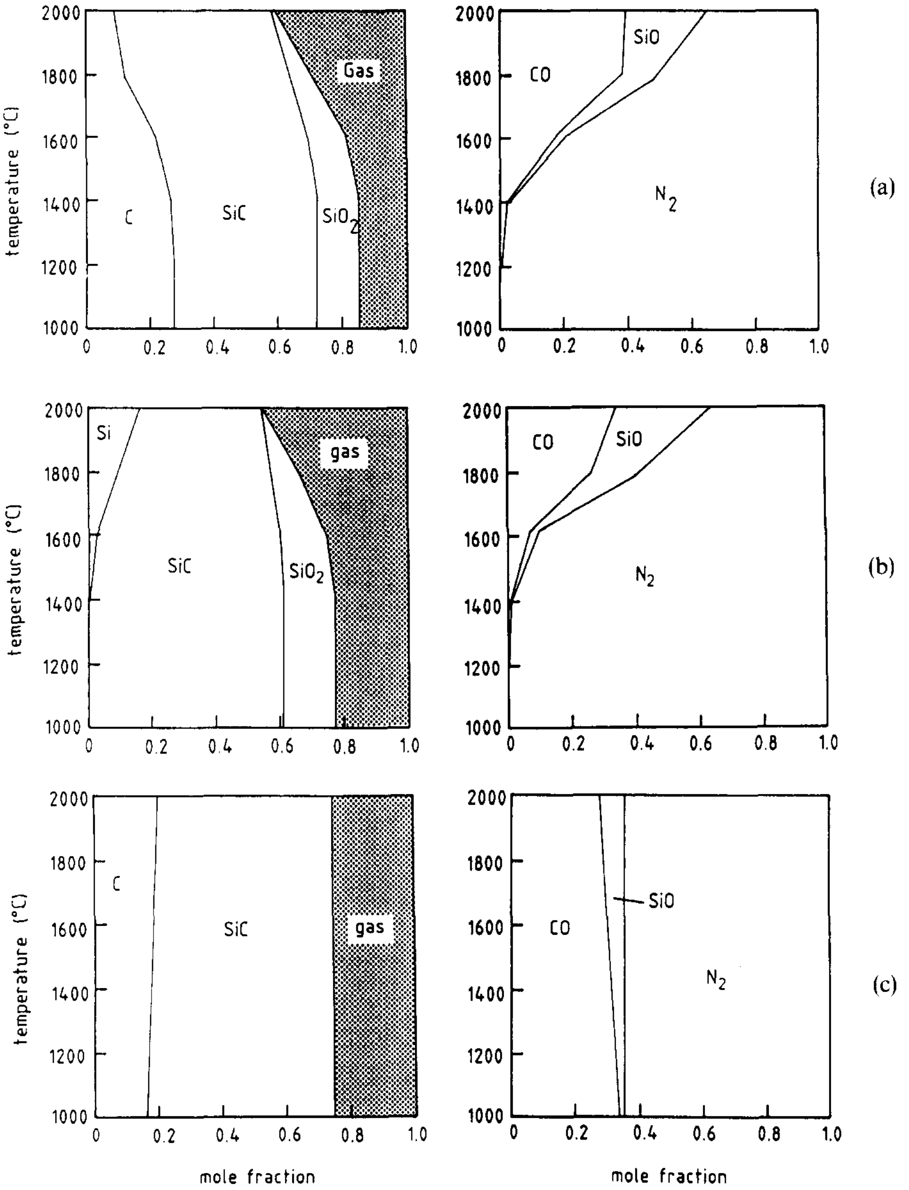

Fig. 2. Phase amount diagrams of the overall phase composition (left) and gaseous phase composition (right) of Si–C–O fibers in air. (a) $3{\cdot}8\,SiC + 1{\cdot}8\,C + 0{\cdot}7\,SiO_2 + 1{\cdot}1\,N_2 + 0{\cdot}3\,O_2$; (b) $3{\cdot}8\,SiC + 0{\cdot}7\,SiO_2 + 1{\cdot}1\,N_2 + 0{\cdot}3\,O_2$; (c) $3{\cdot}8\,SiC + 1{\cdot}8\,C + 1{\cdot}1\,N_2 + 0{\cdot}3\,O_2$.

1800°C was estimated for the $SiC–SiO_2$ system when free Si was present.

Due to the microstructural changes as a result of the fiber decomposition reactions a severe loss of tensile strength was observed in polycrystalline SiC fibers even at temperatures down to 600°C.[18,29–31] The strength loss attained more than one half of the initial value after annealing in Ar or vacuum at temperatures above 1200°C. At these temperatures beginning of surface pitting and grain growth of β-SiC in the outer section of the fiber was observed,[16] which may be associated to the evaporation of CO and SiO from the surface, as indicated by a significant weight loss of more than 5 wt%[29] and by the results of the thermodynamic calculations. Volatization of the fiber and hence microstructural changes may be significantly reduced up to 1300°C by coating the fiber with a thin layer (0·1–0·2 μm) of BN which prevents gas evolution from the fiber surface.[32] High pressure treatment (> 100 MPa) in Ar delayed fiber weight loss to temperatures above 1500°C, which was related to a closure of surface related porosity in the fiber[18] and hence a reduction of the free surface exposed to the gaseous environment.

Figure 2((a) to (c)) shows the corresponding diagrams for fiber degradation in air. In contrast to the inert Ar-atmosphere all fiber compositions are suggested to be unstable in air. The oxygen-free fiber (Fig. 2(c)) decomposes already below 1000°C with CO being the major gaseous species

$$2\langle C\rangle + (O_2) \rightarrow 2(CO) \qquad (10)$$

With increasing temperature the fraction of SiO in the gas phase and residual C in the condensed phase increase, indicating the silicon carbide oxidation reaction

$$\langle SiC\rangle + (O_2) \rightarrow (CO) + (SiO) \quad (11)$$

Figure 2((a) and (b)) indicates a severe degradation reaction to occur in the oxygen containing fibers above 1400°C according to eqn (7) in the free carbon and in the SiO_2-containing fibers:

$$3\langle SiC\rangle + \langle SiO_2\rangle + \tfrac{5}{2}(O_2) \rightarrow 4(SiO) + 3(CO) \quad (12)$$

Both oxidation reactions (11) and (12) describe active oxidation which may occur at low oxygen partial pressures ($<10^{-4}$ MPa at 1400°C).[33] Supplying a higher proportion of air in the starting mixture, however, will result in passive oxidation

$$2\langle SiC\rangle + 3(O_2) \rightarrow 2\langle SiO_2\rangle + 2(CO) \quad (13)$$

and the formation of condensed SiO_2 on the fiber surface instead of gaseous SiO.[34] Thus, surface damage due to gas evaporation may be reduced or even avoided, which is confirmed by annealing experiments of Nicalon fibers in air, where no severe loss of strength was observed.[16] A protective surface layer of amorphous SiO_2 was expected to form above 1300°C which suppresses CO evolution in the fiber. At lower temperatures, however, a protective SiO_2 layer does not form, the CO escapes freely from the surface which results in severe loss of strength.[16] When SiC yarn was exposed to air at 1300°C, a similar loss of strength of more than 50% of the room temperature value was observed, and crystalline cristobalite was identified in the surface layer. During cooling surface cracking may occur due to the volume change when β–α cristobalite phase transformation takes place and due to the differences in thermal expansion coefficient between the oxide ($12{\cdot}5 \times 10^{-6}\,K^{-1}$) and the bulk fiber ($\approx 3$–$3{\cdot}5 \times 10^{-6}\,K^{-1}$).[29]

Based on experimental observations a series of degradation processes was expected to occur during heat treatment.[16] In addition to grain growth and oxidation in air, reaction–dissociation was observed even in inert atmosphere, which may well be explained by the thermodynamic calculations. Exposure of the fiber to any environment whether gaseous or condensed, containing lower partial pressures of CO and SiO than those resulting from reactions (7) to (13) will result in an evolution of these gases from the fiber. At high enough temperatures the gas may leak along the fiber–matrix interface or may even induce cracks in the matrix.[27]

From the calculations it may be concluded that multiphase fiber compositions in the system Si–C–O and in particular those containing free carbon are inherently unstable in air at temperatures above 1000°C. Elimination of O in the fiber composition also excludes the evolution of CO and SiO and hence the oxygen-free SiC–C fiber may be fabricated in Ar atmosphere even at higher temperatures, whereas the manufacturing temperatures of the oxygen-containing fibers must be kept below 1000°C to maintain the initial phase composition. On the other hand, elimination of excess free C would result in a reduction of the CO partial pressure by two orders of magnitude; the partial pressure of SiO would, however, increase by about one order of magnitude.[27] Thus, no significant improvement of thermal stability may be obtained as long as free C or O or both are present. Due to the lack of intrinsic degradation reactions single phase SiC or C fibers seem therefore to promise better stability at elevated fabrication temperatures in inert atmosphere.

3.2 Fiber–matrix reactions

The interface structure between the fiber and the matrix may be severely changed by univariant fiber–matrix reactions during high-temperature fabrication or long exposure to elevated temperatures in service. During fabrication porosity may be retained in the matrix or cracking may occur

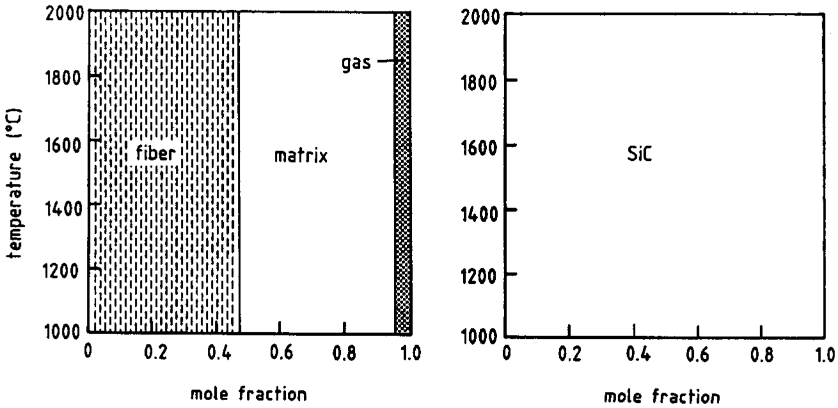

Fig. 3. Phase amount diagrams of C fiber in SiC matrix in the presence of Ar with the overall phases (C + SiC + 0·1 Ar) (left) and the matrix phase (SiC) (right).

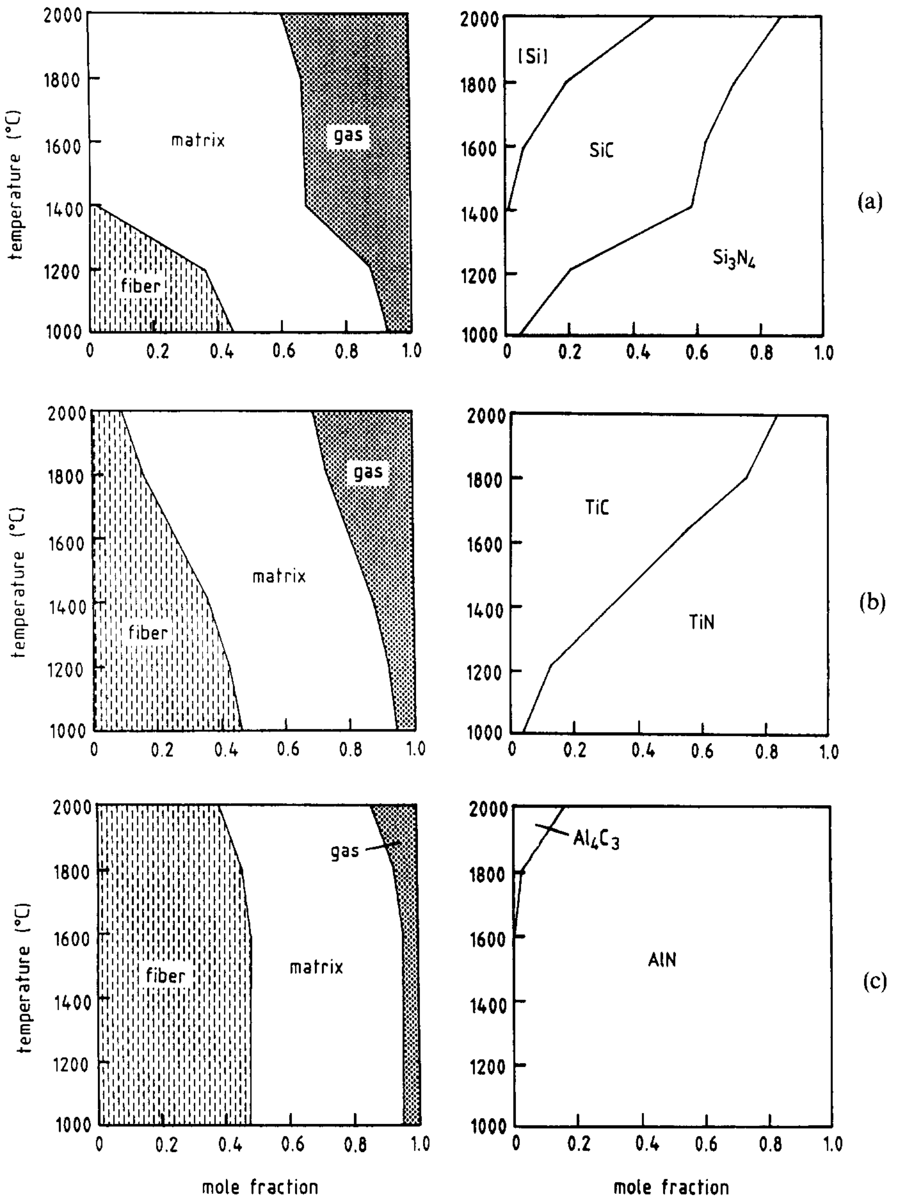

Fig. 4. C fiber in nitride matrices with the overall phases (left) and the matrix phase (right). (a) C + Si_3N_4 + 0·1 Ar; (b) C + TiN + 0·1 Ar; (c) C + AlN + 0·1 Ar.

so that the gas phase should also be included in the equilibria calculations of the fiber–matrix systems. Figure 3 shows that the C–SiC combination is stable in Ar over the whole temperature range. C may therefore also be used as a stable coating on SiC fibers to promote a low-friction interface which results in high composite fracture toughness due to fiber pull out.[35] On the other hand, a SiC coating may serve as an oxidation protection on the C fiber when exposed to air.[17,28] Using C as an intermediate layer on SiC fibers, however, resulted in severe loss of strength of the composite when exposed to high-temperature oxidative conditions, which was related to the non-uniform burnout of the carbon.[36]

3.2.1 C fiber

Due to the fiber stability in carbide matrices SiC and TiC were used as matrices[17,37] as well as coatings to protect the C fiber from reaction with liquid Si.[17] In contrast to the C fiber stability in the SiC matrix, severe fiber–matrix reactions take place with nitride matrices (Fig. 4(a) to (c)). The lowest stability is observed in Si_3N_4 matrix, where SiC may form at the interface and N_2 gas is released at temperatures below 1000°C:

$$3\langle C\rangle + \langle Si_3N_4\rangle \rightarrow 3\langle SiC\rangle + 2(N_2) \qquad (14)$$

Replacing the Ar by N_2 in the atmosphere, however, will stabilize C to higher processing temperatures with increasing N_2 pressure. For example, at 2000°C a N_2 pressure of approximately 10 MPa was calculated to shift the equilibrium to the left side of eqn (14).[38] In spite of the low stability (in Ar) Si_3N_4 has successfully been used as an oxidation protec-

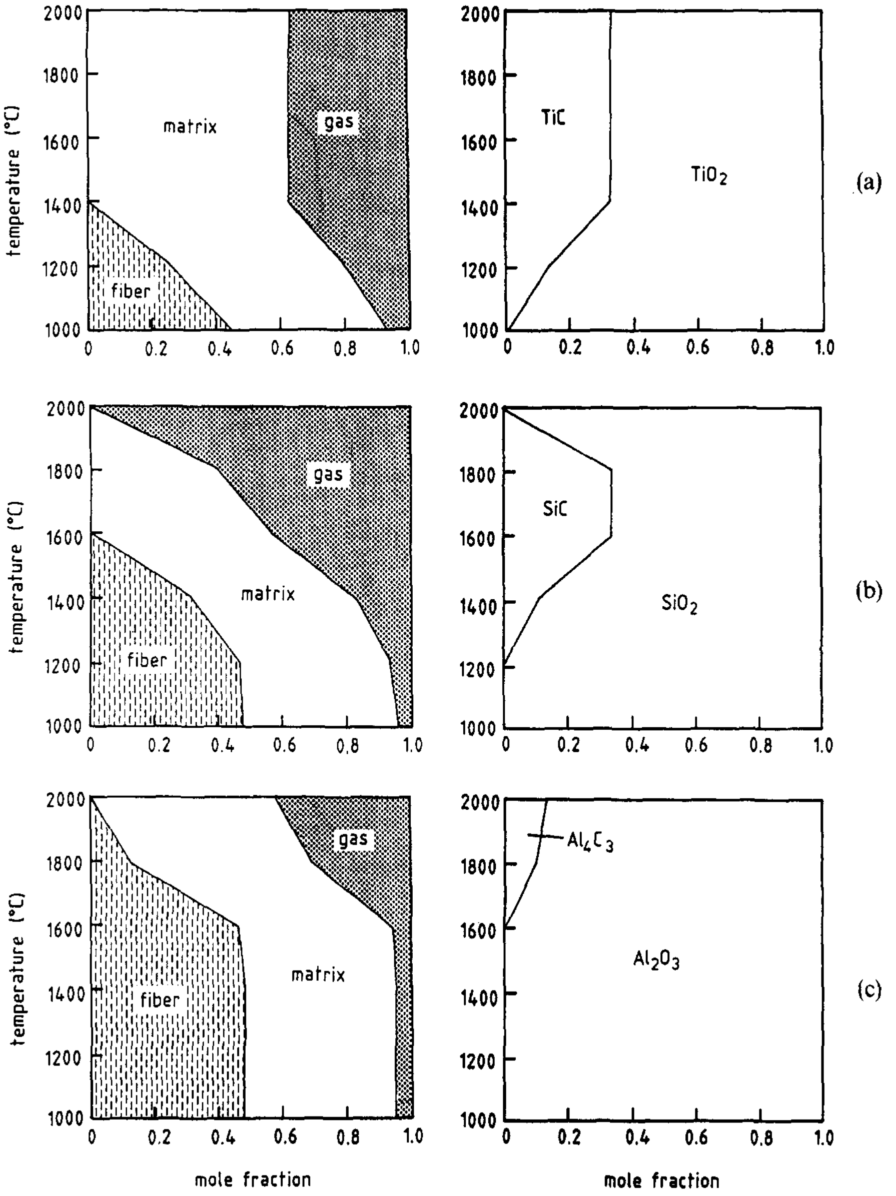

Fig. 5. C fiber in oxide matrices with the overall phases (left) and the matrix phase (right). (a) $C + TiO_2 + 0{\cdot}1\ Ar$; (b) $C + SiO_2 + 0{\cdot}1\ Ar$; (c) $C + Al_2O_3 + 0{\cdot}1\ Ar$.

tion on carbon fiber structures up to more than 1500°C by forming a self-generating $C\text{–}Si_3N_4\text{–}SiO_2$ multilayer structure in air.[28]

A similar fiber–matrix reaction occurs in TiN matrix where TiC is formed at the interface

$$2\langle C\rangle + 2\langle TiN\rangle \rightarrow 2\langle TiC\rangle + (N_2) \qquad (15)$$

Figure 4(b) shows that TiN, which has been discussed as a refractory surface coating on C,[17] may form a reaction interface layer of TiC. In the AlN matrix a significant interface carbide formation is observed only at temperatures above 1600°C

$$3\langle C\rangle + 4\langle AlN\rangle \rightarrow \langle Al_4C_3\rangle + 2(N_2) \qquad (16)$$

indicating the relative stability of the C–AlN system at intermediate temperatures. Although Fig. 4((a) to (c)) suggests severe fiber–matrix reactions in C–nitride systems to occur, the reaction may be shifted to higher temperatures or even suppressed when N_2 release is hindered in high-density materials. Fabrication of these composites is therefore carried out in N_2 atmosphere to stabilize the educts.

Using the nitrides as potential coating material on the C fiber is mainly determined by the pressure of the nitrogen which is formed. Depending on the porosity and mechanical strength of the coating layer cracking may be expected when the gas pressure significantly exceeds the ambient pressure. Nitrogen pressures $>0{\cdot}1$ MPa are calculated to occur at ~1450°C, ~1615°C and ~2540°C (this is the decomposition temperature of AlN at 0·1 MPa) for the reactions (14) to (16), respectively.

Figure 5((a) to (c)) shows the fiber–matrix reactions in the C–oxide systems. Again metal carbides

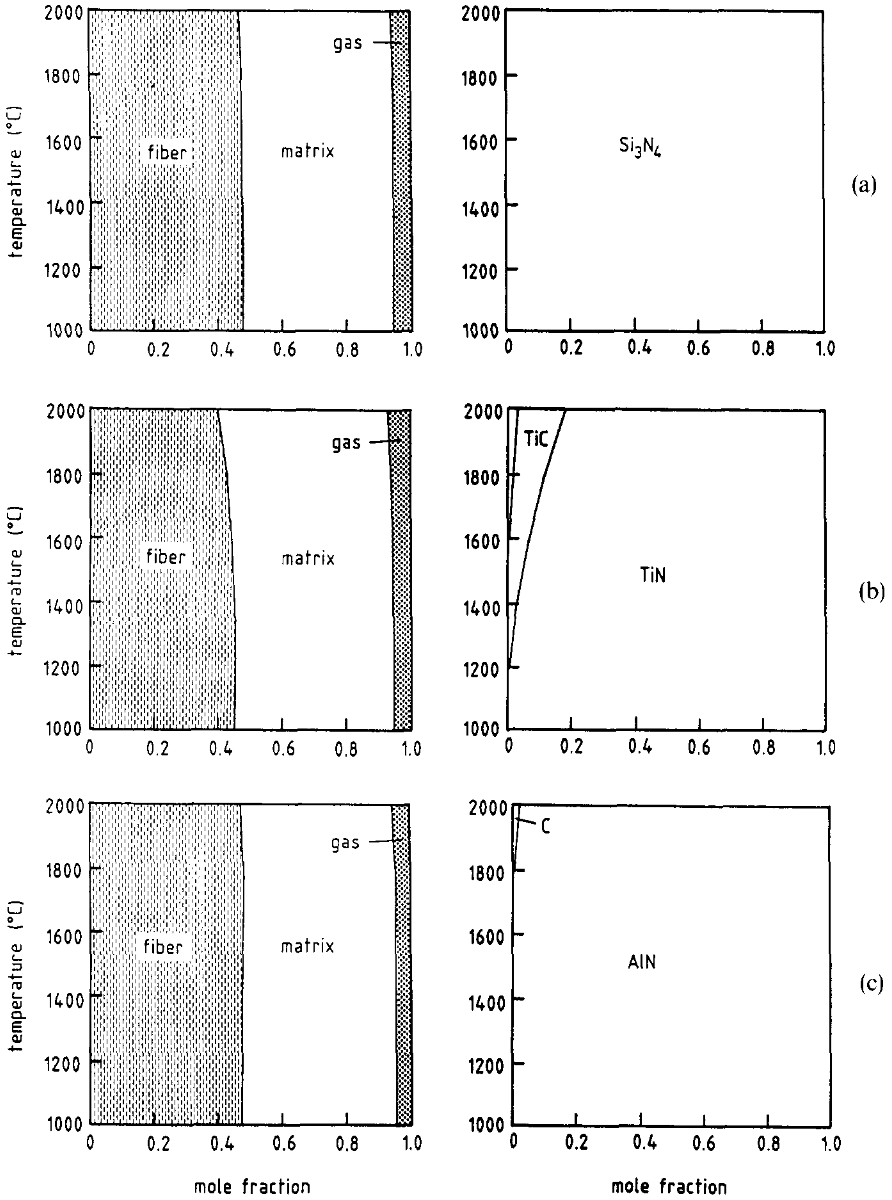

Fig. 6. SiC fiber in nitride matrices with the overall phases (left) and the matrix phase (right). (a) SiC + Si_3N_4 + 0·1 Ar; (b) SiC + TiN + 0·1 Ar; (c) SiC + AlN + 0·1 Ar.

are formed at the interface as the primary condensed reaction products and CO in the gas phase. The C fiber is unstable in TiO_2 and SiO_2 matrices:

$$3\langle C\rangle + \langle TiO_2\rangle \rightarrow \langle TiC\rangle + 2(CO) \quad (17)$$

$$3\langle C\rangle + \langle SiO_2\rangle \rightarrow \langle SiC\rangle + 2(CO) \quad (18)$$

The reduction of TiO_2 and SiO_2 by C produces CO pressures $>0{\cdot}1$ MPa at ~1300°C and ~1510°C, respectively.

The equivalent interface reaction in the Al_2O_3 matrix is suggested to become important above 1600°C

$$9\langle C\rangle + 2\langle Al_2O_3\rangle \rightarrow \langle Al_4C_3\rangle + 6(CO) \quad (19)$$

with a critical gas pressure at ~1730°C. Although this simple calculation encompasses too many facets to be considered in detail here, two facets can be singled out for comment. First, all C–nitride and C–oxide reactions involve the release of gaseous N_2 and CO, respectively, and are therefore dependent on the external atmosphere, the gas pressure and the porosity of the composite materials. Second, stable C–ceramic matrix materials may only be obtained with AlN and Al_2O_3 up to approximately 1600°C. The stability as deduced for inert Ar atmosphere, however, may be reduced significantly in oxidizing atmosphere, so that Figs 3 and 4 only refer to the fabrication and not to the service conditions.

3.2.2 SiC fiber

While high-purity single-phase SiC fibers are not yet available (Table 1) short, single-crystal SiC whiskers have been developed and used as reinforcements in various ceramic matrix systems. Thus, the calculated

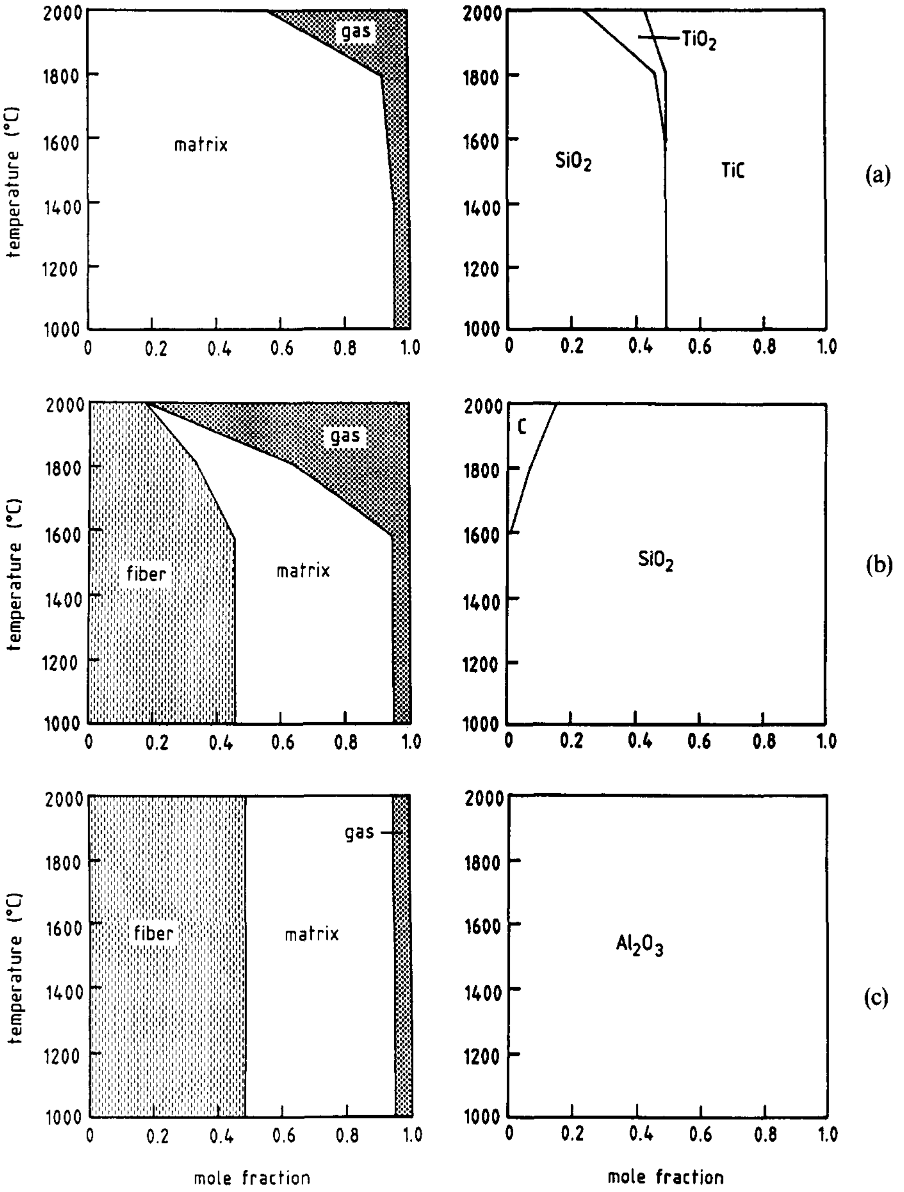

Fig. 7. SiC fiber in oxide matrices with the overall phases (left) and the matrix phase (right). (a) $SiC + TiO_2 + 0{\cdot}1$ Ar; (b) $SiC + SiO_2 + 0{\cdot}1$ Ar; (c) $SiC + Al_2O_3 + 0{\cdot}1$ Ar.

SiC-matrix reactions may be compared to the experimental observations obtained in various SiC–ceramic matrix systems.[38–40] Figure 6((a) to (c)) show the phase diagrams for the SiC–nitride matrix systems. SiC remains stable up to very high temperatures in Si_3N_4 and AlN matrices. In TiN matrix TiC is formed to a higher extent above 1200°C

$$4\langle SiC\rangle + 4\langle TiN\rangle \rightarrow 4\langle TiC\rangle + \langle Si_3N_4\rangle + [Si] \quad (20)$$

In oxide matrices (Fig. 7) the SiC fiber shows no stability in TiO_2:

$$\langle SiC\rangle + \langle TiO_2\rangle \rightarrow \langle TiC\rangle + \langle SiO_2\rangle \quad (21)$$

but remains stable in SiO_2 up to 1600°C where the reaction

$$\langle SiC\rangle + \langle SiO_2\rangle \rightarrow \langle C\rangle + 2(SiO) \quad (22)$$

results in the formation of gaseous SiO as the major decomposition product but with a low gas pressure of $<3\times10^{-5}$ MPa at 1600°C. In various SiC–silicate systems a thin C layer could also be identified at the fiber–matrix interface.[35,41] No interfacial reaction could be detected by TEM analyses in pure Al_2O_3 matrix processed at 1950°C for 1 h[39] and Al_2O_3 sintered with MgO and Y_2O_3 up to 1800°C,[42] whereas in $MgO.Al_2O_3$ (spinel) matrix the formation of $4MgO.5Al_2O_3.2SiO_2$ (saphrine) was observed.[43]

As compared to the C fiber–ceramic matrix composites the SiC fiber composites generally show a better stability towards higher fabrication temperatures. In particular the SiC–AlN and SiC–Si_3N_4 systems may be manufactured even at high temperatures, whereas, except for C–AlN, the nitride matrices are suggested not to be suitable matrices in C fiber-reinforced ceramic matrix composites. An Al_2O_3 matrix, however, may be suitable for both the SiC and the C fibers when the processing temperatures can be kept low, as with the matrix formation via sol–gel transformation.

4 Conclusions

Based on the calculation of the equilibrium composition of multiphase and multicomponent systems case studies on potential fiber degradation reactions in gaseous and condensed environment are described. Though the reaction kinetics may exert a significant influence on the degree of microstructural change in the fiber and at the fiber–matrix interface the equilibrium calculations may provide information on the inherent stability or instability of a particular fiber or fiber–matrix system under specific environmental conditions.

Polycrystalline Si–C–O fibers show severe loss of strength at high temperatures which can be attributed to internal thermochemical degradation reactions between the fiber constituents as well as to external reactions with the atmosphere. Evolution of gas species (mainly CO and SiO) from the surface of the fibers may occur at temperatures even below 1000°C and results in significant microstructural changes at the outer fiber zone. The inherent thermodynamic instability of C and SiC in oxide systems (and in oxidizing conditions) renders fiber degradation a time- and temperature-dependent kinetic phenomenon that can be hindered but not eliminated.

To avoid fiber degradation during processing the fabrication temperatures have to be significantly reduced ($<1000°C$) or the high-temperature stability of the fibers has to be improved. Closure of surface-related porosity by high-pressure treatment was shown to shift the degradation reactions to higher temperatures, indicating the significance of fiber surface morphology for thermochemical degradation. The development of appropriate high temperature stable fiber coatings is probably an easier method to achieve environmentally stable fiber–matrix interfaces up to higher processing temperatures ($>1200°C$). Fiber coatings to inhibit fiber volatilization should therefore be chemically compatible to the fiber, like the carbides and some nitrides, or have to provide sufficient density and mechanical strength to sustain the gas pressure which may be generated at the fiber-coating interface during high-temperature processing.

Thus, boundary conditions for improved processing and use of fiber-reinforced ceramic composites may be derived from the thermodynamic equilibrium calculation approach. Extension of the calculations to other fiber–matrix systems including impurities present at the interface is recommended highly in order to understand the material behavior under severe environmental conditions, to exclude unreasonable material combinations and to develop improved fiber coatings.

Acknowledgment

K. G. Nickel, MPI for Metals Research Stuttgart, is gratefully acknowledged for helpful discussion.

References

1. Prewo, K. M., Fiber-reinforced ceramics: New opportunities for composite materials. *Am. Ceram. Bull.*, **68** (1989) 395.
2. Yajima, S., Okamura, K., Hayashi, J. & Omori, M. Synthesis of continuous SiC fibers with high tensile strength. *J. Am. Ceram. Soc.*, **59** (1976) 324.
3. Mah, T.-I., Mendiratta, M. G., Katz, A. P. & Mazdiyasni, K. S., Recent developments in fiber-reinforced high-temperature ceramic composites. *Am. Ceram. Soc. Bull.*, **66** (1987) 304.
4. Prewo, K. M. & Brennan, J. J., High strength silicon carbide fiber-reinforced glass-matrix composites. *J. Mat. Sci.*, **15** (1980) 463.
5. Prewo, K. M. & Brennan, J. J., Silicon carbide yarn-reinforced glass-matrix composites. *J. Mat. Sci.*, **17** (1982) 1201.
6. Brennan, J. J. & Prewo, K. M., Silicon carbide fiber-reinforced glass-ceramic matrix composites exhibiting high strength and toughness. *J. Mat. Sci.*, **17** (1982) 2371.
7. Lamicq, P. J., Bernhart, G. A., Dauchier, M. M. & Mace, J. G., SiC/SiC composite ceramics. *Am. Ceram. Bull.*, **65** (1986) 336.
8. Cornie, J. A., Chiang, Y. M., Uhlmann, D. R., Mortensen, A. & Collins, J. M., Processing of metal and ceramic matrix composites. *Am. Ceram. Bull.*, **65** (1986) 293.
9. Rice, R. W., Spann, J. R., Lewis, D. L. & Coblenz, W. S., The effect of ceramic fiber coatings on the room-temperature mechanical behavior of ceramic–fiber composites. *Ceram. Eng. Sci. Proc.*, **5** (1984) 614.
10. Faber, K. T., Advani, S. H., Lee, J. K. & Jinn, J. T., Frictional stress evaluation along the fiber–matrix interface in ceramic matrix composites. *J. Am. Ceram. Soc.*, **69** (1986) C-208.
11. Goettler, R. W. & Faber, K. T., Interfacial shear stresses in SiC- and Al_2O_3-fiber-reinforced glasses. *Ceram. Eng. Sci. Proc.*, **9** (1988) 861.
12. Brun, M. K. & Singh, R. N., Effect of thermal expansion mismatch and fiber coating on the fiber/matrix interfacial shear stress in ceramic matrix composites. *Adv. Ceram. Mat.*, **3** (1988) 506.
13. Cranmer, D. C., Fiber coating and characterization. *Am. Ceram. Bull.*, **68** (1989) 415.
14. Bender, B., Shadwell, D., Bulik, C., Incorvati, L. & Lewis III, D., Effect of fiber coatings and composite processing on properties of zirconia-based matrix SiC fiber composites. *Am. Ceram. Soc.*, **65** (1986) 363.
15. Singh, R. N. & Brun, M. K., Effect of boron nitride coating

on fiber–matrix interactions. *Ceram. Eng. Sci. Proc.*, **8** (1987) 636.

16. Mah, T., Hecht, N. L., McCullum, D. E., Hoenigmann, J. R., Kim, H. M., Katz, A. P. & Lipsitt, H. A., Thermal stability of SiC-fibers (Nicalon). *J. Mat. Sci.*, **19** (1984) 1191.
17. Fitzer, E. & Gadow, R., Fiber-Reinforced silicon carbide. *Am. Ceram. Bull.*, **65** (1986) 326.
18. Jaskowiak, H. M. & Dilarlo, J. A., Pressure effects on the thermal stability of silicon carbide fibers. *J. Am. Ceram. Soc.*, **72** (1989) 192.
19. Benson, P. M., Spear, K. E. & Pantano, C. G., Interfacial characterization of glass matrix/Nicalon SiC fiber composites: A thermodynamic approach. *Ceram. Eng. Sci. Proc.*, **9** (1988) 663.
20. Spear, K. E., Benson, P. M. & Pantano, C. G., Thermochemical modeling for interface reactions in carbon-fiber-reinforced glass-matrix composites. In *Proc. of the Electrochem. Soc. 88-5*. Electrochemical Society, NY, 1988, p. 345.
21. Mendelson, M. I., SiC/Glass composite interphases. *Ceram. Eng. Sci. Proc.*, **6** (1985) 612.
22. Zeitler, M., Schmidt, W., Wittig, B., Goldhammer, W., Barin, I., Eriksson, G. & Sauert, F., *Equitherm: Datenbank und Programm für Thermodynamische Berechnungen*. VCH Verlagsgesellschaft, Weinheim, FRG, 1989.
23. Eriksson, G., Thermodynamic studies of high temperature equilibria. *Chem. Scripta*, **8** (1975) 100.
24. Leitner, J., Vonka, P. & Mikulec, J., Review: Application of chemical thermodynamics to the description of processes of special inorganic materials preparation. *J. Mat. Sci.*, **27** (1989) 1521.
25. Barin, I., *Thermochemical Data of Pure Substances*. VCH Verlagsgesellschaft, Weinheim, FRG, 1989.
26. Lukas, H. L., Weiss, J. & Henig, E. T., Strategies for the calculation of phase diagrams. *CALPHAD*, **6** (1982) 229.
27. Luthra, K. L., Thermochemical analysis of the stability of continuous 'SiC' fibers. *J. Am. Ceram. Soc.*, **69** (1986) C-231.
28. Strife, J. R. & Shechan, J. E., Ceramic coatings for carbon–carbon composites. *Am. Ceram. Soc. Bull.*, **67** (1988) 369.
29. Fareed, A. S., Fang, P., Koczak, M. J. & Ko, F. M., Thermomechanical properties of SiC yarn. *Am. Ceram. Soc. Bull.*, **66** (1987) 353.
30. Stinton, D. P., Caputo, A. J. & Lowden, R. A., Synthesis of fiber-reinforced SiC composites by chemical vapor infiltration. *Am. Ceram. Soc. Bull.*, **65** (1986) 347.
31. Pysher, D. J., Goretta, K. C., Hodder, R. S. & Tressler, R. E., Strengths of ceramic fibers at elevated temperatures. *J. Am. Ceram. Soc.*, **72** (1989) 284.
32. Bender, B., Shadwell, D., Bulik, C., Incorvati, L. & Lewis III, D., Effect of fiber coatings and composite processing on properties of zirconia-based matrix SiC-fiber composites. *Am. Ceram. Bull.*, **65** (1986) 363.
33. Singhal, S. C., Thermodynamic analysis of the high temperature stability of silicon nitride and silicon carbide. *Ceramurgia Intern.*, **2** (1976) 123.
34. Warren, R. & Andersson, C. M., Silicon carbide fibers and their potential for use in composite materials, Part II. *Composites*, **15** (1984) 101.
35. Herron, M. A. & Risbud, S. H., Characterization of SiC-fiber-reinforced Ba–Si–Al–O–N glass-Ceramic Composites. *Am. Ceram. Bull*, **65** (1986) 342.
36. Caputo, A. J., Stinton, D. P., Lowden, R. A. & Besmann, T. M., Fiber-reinforced SiC composites with improved mechanical properties. *Am. Ceram. Soc. Bull.*, **66** (1987) 368.
37. Naslain, R., Synthesis and properties of new composite materials for high temperature applications based on carbon fibers and C/SiC or C/TiC. *Rev. Chim. Minerale*, **18** (1981) 544.
38. Nickel, K. G., Hoffmann, M. J., Greil, P. & Petzow, G., Thermodynamic calculations for the formation of SiC-whisker-reinforced Si_3N_4-ceramics. *Adv. Ceram. Mat.*, **3** (1988) 557.
39. Homeny, J., Vaughn, W. L. & Ferber, M. K., Processing and mechanical properties of SiC-whisker–Al_2O_3-matrix composites. *Am. Ceram. Soc. Bull.*, **67** (1987) 333.
40. Wei, G. C. & Becher, P. F., Development of SiC-whisker reinforced ceramics. *Am. Ceram. Soc. Bull.*, **64** (1985) 298.
41. Chaim, R. & Heuer, A. H., The interface between Nicalon SiC fibers and a glass-ceramic matrix. *Adv. Ceram. Mat.*, **2** (1987) 154.
42. Tiegs, T. N. & Becher, P. F., Sintered Al_2O_3–SiC-whisker composites. *Am. Ceram. Soc. Bull.*, **66** (1987) 339.
43. Panda, P. C. & Seydel, E. R., Near-net-shape forming of magnesia spinel/silicon carbide fiber-composites. *Am. Ceram. Soc. Bull.*, **65** (1986) 338.
44. Legrow, G. E., Lim, T. F., Lipowitz, J. & Reaoch, R. S., Ceramics from hydridopolysilazane. *Am. Ceram. Soc. Bull.*, **66** (1987) 363.